# Examination of Internal Reflection Method in Visible Region and Application to Electrochemistry



Fujinaga, Taitiro; Kuwamoto, Tooru; Hinoue, Teruo

Bull. Inst. Chem. Res., Kyoto Univ., Vol. 54, No. 5, 1976

# Examination of Internal Reflection Method in Visible Region and Application to Electrochemistry

Taitiro FUJINAGA, Tooru KUWAMOTO, and Teruo HINOUE*

*Received August 2, 1976*

In order to investigate the electrochemical reactions by means of the internal reflection method in the visible region, an optical system and accessories for the method were designed and settled in the sample compartment of the commercial spectrophotometer. By using this system, the internal reflection spectra (ATR spectra) of permanganate solutions were measured. As the results, the "effective thickness" and the number of the total reflections of the optical system were determined as $1.5 \times 10^4/A^0$ and four times, respectively, according to Hansen's theory. The proportionality between the "effective thickness" and the wavelength was also confirmed as expected from Hansen's equations. From these facts, Hansen's theory was proved to hold in our internal reflection system. According to this confidence, the internal reflection system was applicable to monitoring the anodic oxidation of 0-Tolidine in acidic solutions by using an optical transparent electrode, which was a quartz prism plate covered with gold. The change of the reflection absorbance at 437 nm due to the oxidation product of 0-Tolidine was monitored versus time. The results agreed qualitatively with the Kuwana's theory, which explains the mass transfer processes caused by the electrochemical perturbation.

## INTRODUCTION

It is known that some of heterogeneous catalytic reactions and adsorption equilibria on colloidal particles relate closely to solid-liquid interfacial phenomena. The interfacial phenomena have been broadly studied in the field of colloidal chemistry and electrochemistry, especially, in electrochemistry, the mechanism study of electrode-solution interface has been interested in relation to the electrode processed. However, it has been hardly possible to observe the interface directly and characterize it more microscopically, because of the lack of suitable methodologies. Recently, Harrick succeeded[1] in the measurement of infrared spectra of the thin layer consisted of water and/or polyethylene molecules oriented on germanium plate by means of the internal reflection method. Fahrenfort obtained[2] infrared spectra of organic materials on silver chloride plate using the similar method. These were the first attempt for the direct investigation or optical observation of the interfaces. Harrick[3] and Hansen[4] studied the optics of the thin stracked layers on a transparent substrate and derived general equations for the internal reflection in the ideal system. Thanks to these developments of the internal reflection method has proved itself an extremely valuable method for the observation of the interfaces in situ. Then the method has been extended to the visible region.[5~8] In the applications of the method to electrochemistry, many important intermediates generated in the course of electrode processes were identified.[6,9] With the internal reflection method in visible

* 藤永太一郎，桑本　融，樋上照男：Department of Chemistry, Faculty of Science, Kyoto University, Kyoto, 606.

region, Kuwana and co-workers investigated mass transfer processes in combination with various electrochemical perturbation.

In the present work, the authors designed an optical system for the internal reflection method which enables as to measure internal reflection spectra (Attenuated Total Reflection Spectra) of visible region. The optical system was calibrated by using the absorption spectrum of permanganate solution as the standard and thereby the optical constants of this system were determined. An optical transparent electrode made with a quartz plate covered with gold has been prepared and the mechanism of the electrode reaction of 0-Tolidine at the anodic process was investigated in acidic solutions.

## EXPERIMENTS

### 1 The Cell for the Internal Reflection Method

Figure 1 shows each part of the used cell for the internal reflection system. The cell is essencially similar to that designed by Tallant and Evans,[6] but different from the germanium prism used by them, the present authors used the quartz prism plate, because it is necessary in the present method of the internal reflection to cover the wavelength of visible region. The size of this prism plate is 20 mm × 72 mm × 1 mm and its shape in the 1 mm × 72 mm plane is the regular trapezoid with the bottom angle of 60°. This prism plate was held in the middle of the half vessels made of tefron and fixed by Araldite.

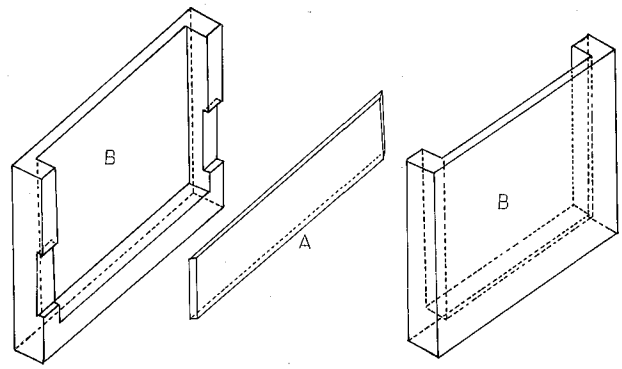


Fig. 1 Cell for measuring the internal reflection spectra. A; quartz prism plate, B; half vessel made of tefron

### 2 The Preparation of an Optical Transparent Electrode and the Electrochemical Apparatus

In the electrochemical experiment using the internal reflection method, the cell used was similar to that shown in Fig. 1, but instead of the quartz prism plate, an optical transparent electrode prism (OTE prism) was set in the cell of the same position as the quartz prism plate. In the electrochemical experiment, OTE prism functioned as a working electrode, SCE as a reference electrode and T-shaped

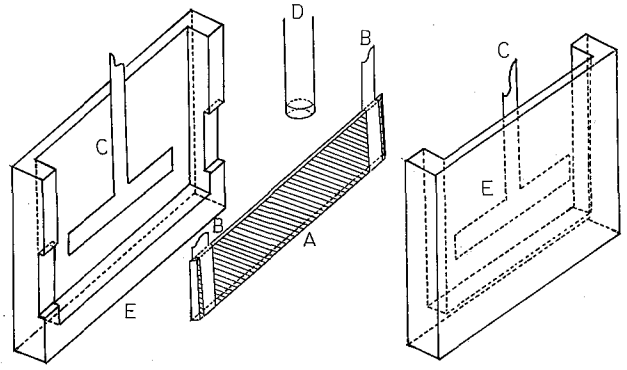


Fig. 2 Cell for the electrochemical experiment by using the internal reflection method.
A; OTE prism plate, B; gold strip for the electric contact with the external circuit, C; counter electrode, D; to the reference electrode, E; half vessel made of tefron

platinium thin plate as a counter electrode. The cell and these electrodes are shown in Fig. 2. OTE prism was prepared by the following procedures. The quartz plate same as mentioned in the previous section, was washed with acetone to remove oily dust and washed with a dilute hydrochloric acid solution and distilled water successively. The plate was dried at room temperature. Nextly, it was covered with chromium metal very thinly and followed with gold metal by the vacuum evaporation. The total thickness of the metallic layers was approximately 200A°.

### 3 The Accessary Optical System for the Internal Reflection Method

The spectrophotometer used was the Shimadzu model UV-200. An accessary optical system for the internal reflection method was designed as fitted with the sample compartment of this spectrophotometer. In order to discuss the design in detail, the behavior of the light beam in the accessary optical system is given in Fig. 3. The black line shown in Fig. 3 gives the behavior. Firstly, the light beam is reflected by the planar mirror (M1) and nextly by the planar mirror (M2). And then the beam enters into the prism plate (or OTE prism) and takes place the total reflection at the boundary between the prism plate and a solution several times. After several reflections, the beam departs from the last plane of the prism plate and is returned to the original optical system of UV-200 by reflecting from the planar mirror (M3) and the concave mirorr (M4). In order to obtain the behavior, there were three problems which had to be considered in designing of this system. The first problem is about the determination of the positions of the mirrors shown as M1 and M2, the second is the determination of the angle between the axis of the light beam and the axis of the prism plate and the third is about returning the departing light beam from the last plane of the prism plate to the original optical system of UV-200. These problems are discussed below in detail.

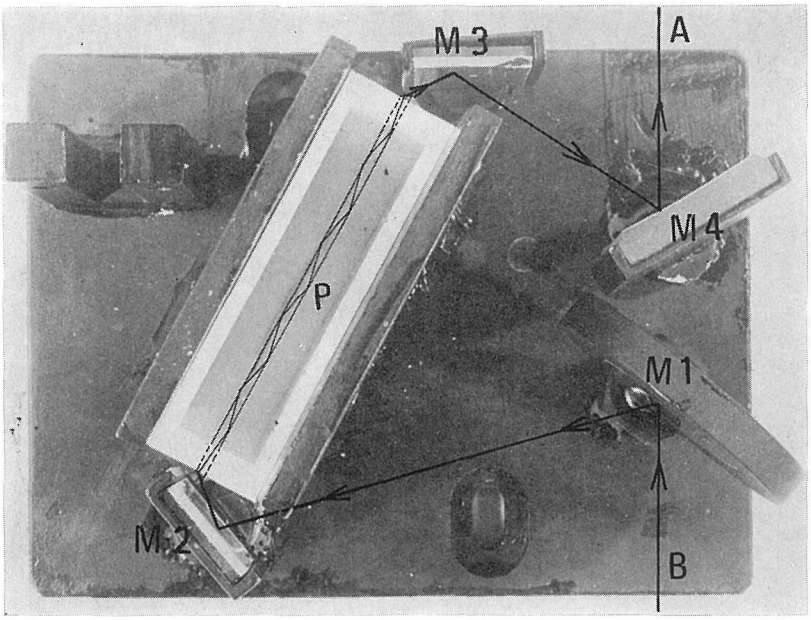


Fig. 3 Accessary optical system for the internal reflection method and the behavior of the light beam in this system.
A; to the detector, B; from the monochrometer, P; prism plate

i) *On the Determination of the Positions of the Mirrors M1, M2*

The width of the incident plane of the prism plate is calculated from the thickness of the prism plate (=1 mm) and the bottom angle of the regular trapezoid (=60°) in the 1 mm×72 mm plane and its value is 1/sin60°=1.15 mm. So in order to let the light beam enter into the prism plate, it is necessary to find the position where the light beam becomes less than 1.15 mm in the original optics of UV-200 and move the incident plane of the prism plate to the position. In Fig. 4, the original optics of UV-200 is shown and the position which the light beam becomes

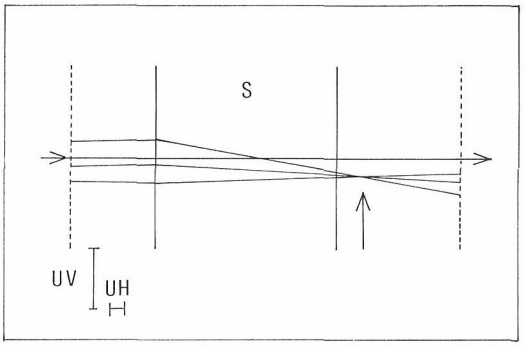


Fig. 4 Optics near the sample compartment of UV-200.
S; sample compartment, UV; 1 cm in the vertical direction, UH; 1 cm in the horizontal direction

less than 1.15 mm is given by an allow. According to the figure, the position is out of the sample compartment. In order to remove this situation and move the position to the sample compartment, two planar mirrors were used.

ii) *On the Determination of the Angle Between the Axis of the Prism Plate and the Axis of the Light Beam*

As the beam in the prism plate must be totally reflected at the boundary between the prism plate and a solution, the incident angle to the boundary must be 65.5° and 90°, as the refractive indices of quartz and water are 1.45 and 1.33 respectively. As the incident angle approaches to 65.5, the number of the total reflections increases, because the distance from one reflection point to the next reflection point becomes shorter. Oppositely as the incident angle approaches to 90°, the number of the total reflections decreases, because the distance between two adjacent points of the total reflections becomes longer. As S/N ratio of the total reflection absorbance is improved, with increasing the number of the total reflections, the former is favored. However, as the light beam from the monochrometer is not collimated completely, the departing beam from the last plane of the prism plate is divergent and the divergence in the former case is more spacious than in the later case. By considering these opposite situations, the incident angle to the boundary was determined as 86.0° and the angle of the axis of the prism plate and the axis of the the light beam was determined as 10°.

iii) *On the Returning of the Departing Beam from the Last Plane of the Prism Plate to the Original Optical System of UV-200*

The departing beam from the last plane of the prism plate was led to the original optical system of UV-200 by reflecting from two mirrors. One is a planar mirror shown as M3 and the other is a concave mirror with the curvature 250 mm in diameter shown as M4 in Fig. 3. The positions of the mirrors were calculated by geometrical optics. After these considerations, the accessary optical system was designed as proper to the sample compartment of UV-200. According to the design, four mirrors and the prism plate held in the cell were arranged in the sample compartment. The total figure of this system is shown in Fig. 3. In the design, the incident angle was 86.0°, but practically there were deviations from the design during manufacturing, the actual incident angle was determined by measuring the scale of the complete optical system and its value was 87.0°. Further, in the experiment, the proper filter for the compensation on the way of the reference beam, because the sample beam was weak.

## 4 The Preparation of Sample Solutions

GR grade potassium permanganate obtained from Nakarai Chemicals Co. was recrystallized from distilled water and dried at room temperature. The sample solutions were freshly prepared by dissolving it into 0.18N-$H_2SO_4$ solutions at each experiment. 0-Tolidine was purified by the following procedure; 0-Tolidine from Tokyo Kasei Chemicals Co. Ltd., was dissolved into a dilute hydrochloric solution.

After dissolution, equivalent amount of a sodium hydroxylic solution was added to let it precipitate quantitatively. The precipitation was washed with distilled water and dried at room temperature. Other reagents were all reagent grade and used without further purification.

## RESULTS AND DISCUSSIONS

The internal reflection spectra (ATR spectra) of potassium permanganate were measured in 0.18N-$H_2SO_4$ solutions and are shown in Fig. 5. In the figure, curve 1 is the base line spectrum and curves 2, 3, 4, and 5 are the spectra of potassium permanganate solutions with respective concentrations of $4.75\times10^{-2}$, $9.50\times10^{-2}$, $1.90\times10^{-1}$, and $3.80\times10^{-1}$M. In all of the spectra of permanganate anions four charac-

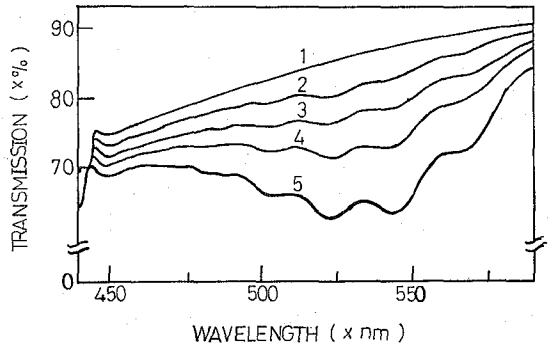


Fig. 5 ATR spectra of potassium permanganate in 0.18N-$H_2SO_4$ solutions, 1; blank, 2; $4.75\times10^{-2}$M, 3; $9.50\times10^{-2}$M, 4; $1.90\times10^{-1}$M, 5; $3.80\times10^{-1}$M, respectively

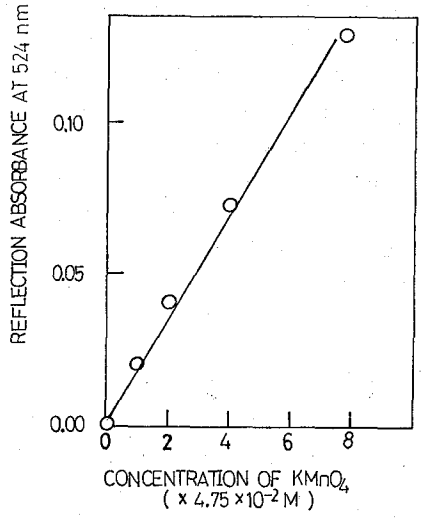


Fig. 6 Dependence of the reflection absorbance on the concentration of potassium permanganate

teristic absorption bands are evidently at 505 nm, 524 nm, 543 nm, and 562 nm. These absorption bands agree well with those observed by the normal transmission spectra of permanganate solutions. This agreement means that the states of permanganate anions on the quartz surface resemble that of permanganate anions in the bulk solution, namely, the permanganate anions are not particularly adsorbed on the quartz surface. In Fig. 6, the dependence of the reflection absorbance on the concentration of the potassium permanganate at 524 nm is shown. In the figure, it is clearly seen that the reflection absorbance proportionally increases, with increasing the concentration of potassium permanganate in the range of $4.75\times10^{-2}$M and $3.80\times10^{-1}$M. This fact can be explained from one of Hansen's equations.[4] The equation gives Beer's law in the internal reflection system, assuming that an attenuation coefficient of a solution phase is less than the unity, and is given

$$A = a\times B_{\text{eff}}\times C \qquad (1)$$

Where $A$ is the reflection absorbance, $a$ is the extinction coefficient and $C$ is the concentration of absorbed species. $B_{\text{eff}}$ is called "effective thickness" and corresponds to the path length in the normal transmission spectroscopy. As $a$ and $B_{\text{eff}}$ are constant at the constant wavelength, the dependence of the reflection absorbance on the concentration obeys this Beer's law shown in Eq. (1). Nextly, according to Eq. (1), $B_{\text{eff}}$ which corresponds to the path length in the normal transmission spectroscopy can be calculated from the slope of the straight line shown in Fig. 6 and its value is $1.5\times10^{4}$A°, as the extinction coefficient of permanganate anions is known as $2.3\times10^{-3}\text{M}^{-1}\,\text{cm}^{-1}$ at 524 nm. On the other hand, $B_{\text{eff}}$ is estimated theoretically as the function of optical parameters and the incident angle in the internal reflection system and the wavelength by Hansen's theory,[4] and is given

$$\text{B}_{\text{eff}} = N\times n_{\text{soln.}}\times[E^2_{\text{soln.}}]^{\circ}\times d/n_q\times\cos\theta_i \qquad (2)$$

$$d = \lambda/4\pi(n_{\text{q}}^2\sin^2\theta_i - n^2_{\text{soln.}})^{1/2} \qquad (3)$$

$$\text{for}\quad k_{\text{soln.}} = 0,\ \theta_i > \theta_c$$

where $n_q$ and $n_{\text{soln.}}$ are refraction indices of the quartz phase and the solution phase respectively. $\theta_i$ and $\theta_c$ are the incident angle and the critical angle in the internal reflection system. $N$ is the number of the total reflections and $\lambda$ is the wavelength in vacuo. $k_{\text{soln.}}$ is the attenuation coefficient and $d$ is called "penetration depth" and is the distance from the boundary between the quartz phase and the solution phase to the point where the time average of amplitude of the electric field strength decreases to $1/e$ of its initial value, when the total reflection takes place at the boundary. $[E^2_{\text{soln.}}]$ is the time average of amplitude of electric field at the boundary, when the solution phase is transparent. From Eqs. (2), (3), $B_{\text{eff}}$ is calculated theoretically and its value is $1.44\times10^{4}$A°, when $N$ is four times, $\lambda$=524 nm, $n_q$=1.45, $n_{\text{soln.}}$=1.33, $\theta_i$=87.0°, $[E^2_{\text{soln.}}]^{0}$=0.3. This theoretical value is agreed with the experimental value ($1.50\times10^{4}$A°).

In the second column of Table I, the absorbances at four maxima in ATR spectrum of the 0.19M-permanganate solution and those in the normal transmission

Table I

| | Wavelength (nm) | Absorbance | Peak ratio $A_{x\,nm}/A_{524\,nm}$ | Corrected peak ratio $A_{x\,nm}/A_{524\,nm} \times X\,nm/524\,nm$ |
|---|---|---|---|---|
| ATR | 505 | 0.0977 | 0.709 | 0.736 |
| | 524 | 0.138 | 1.000 | 1.000 |
| | 543 | 0.141 | 1.020 | 0.984 |
| | 562 | 0.0856 | 0.621 | 0.580 |
| NTS* | 505 | 0.502 | 0.750 | |
| | 524 | 0.669 | 1.000 | |
| | 543 | 0.645 | 0.964 | |
| | 562 | 0.363 | 0.542 | |

* the normal transmission spectroscopy

spectrum of $2.9 \times 10^{-4}$M-permanganate solution are given and in the third column, peak ratios calculated from the absorbances at 524 nm as the standard in both spectra. The comparison of peak ratios of ATR spectrum with those in the normal transmission spectrum gives the fact that peak ratios of ATR spectrum is smaller than that of the normal transmission spectrum at 505 nm in the shorter range of the wavelength than the standard wavelength (=524 nm) and peak ratios of ATR spectrum are larger than those of the normal transmission spectrum in the longer range than the standard wavelength. This fact can be explained by the following consideration. According to Eqs. (2), (3), $B_{eff}$ is proportional to the wavelength, assuming that the other optical parameters in the internal reflection system keep constant, even though the concentration of potassium permanganate changes. On the other hand, in the normal transmission spectroscopy, the path length is kept constant during the measurement of the spectra. This difference of the nature of the path length between both spectroscopies explains the above experimental fact qualitatively. In order to demonstrate that the difference of peak ratios in ATR spectra from those in the normal transmission spectra is due to the proportionality of $B_{eff}$ to the wavelength, the peak ratios at 505, 543, and 562 nm referred to the peak 524 nm in ATR spectra were corrected, assuming that all the three $B_{eff}$ have the same value as that of 524 nm. These corrected peak ratios are given in the fourth column of Table I. The dependence of peak ratios in ATR spectrum on the wavelength is same that of peak ratios in the normal transmission spectrum in the third column and their values agree with those of the normal transmission spectrum within experimental errors. From these results, Hansen's theory are proved to hold in our internal reflection system and it is concluded that $B_{eff}$ is $1.5 \times 10^4$A° and the number of the total reflections is four times.

As it was demonstrated that the experimental results obtained by our internal reflection system agreed with Hansen's theory, this internal reflection system was applied to the investigation of the electrochemical reactions occurring at the vicinity of the solid electrode. This application was tried using an optical transparent electrode instead of the prism plate used in the above experimental work. The double potential step method from 0.00 volt to 0.85 volt *vs.* SCE was used as the

electrochemical method and the reaction monitored by the internal reflection method was the anodic oxidation process of 0-Tolidine. The anodic oxidation process of 0–Tolidine in the acidic solution was examined by the cyclic voltammetry and its voltammogram gives the reversible two-electrons oxidation peak at ca. 0.5 volt *vs.* SCE. And its schematic reaction diagram is given by

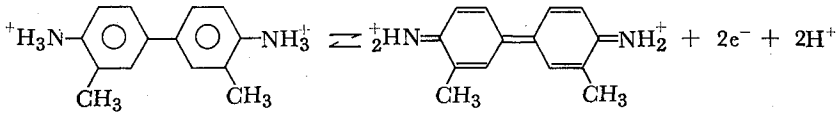

I II

The compound I is protonated 0-Tolidine and the compound II is the oxidation product, which has the absorption maximum at 437 nm. The change of the reflection absorbance at 437 nm was monitored during the electrochemical perturbation caused by the double potential step method. The curves recored in the experiment are shown in Fig. 7. Curve 1 shows the chronological change of the reflection absorbance with a new sample solution and curves 2 and 3 show the similar absorbance change after repeated electrolysis. The reflection absorbances in all of the curves attain the constant value after several seconds from the potential step from 0.00 volt to 0.85 volt *vs.* SCE. The behavior of the reflection absorbance in the internal reflection system was expected by one of Kuwana's equations[10] According to the equation, the reflection absorbance attains the constant value within 1 ms. Our experimental results agree with Kuwana's expectation in respect to the saturation of the absorbance after several seconds from the potential step, however the experi-

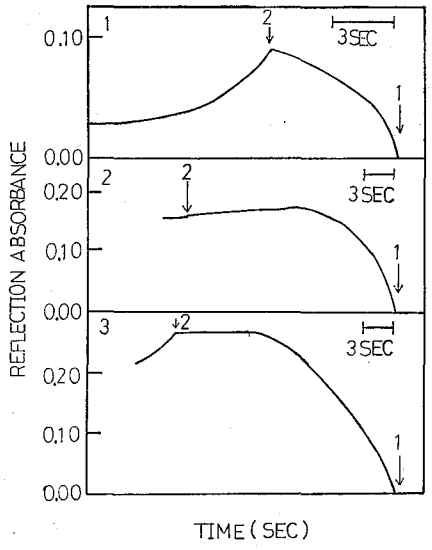


Fig. 7 Chronological change of the reflection absorbance at 437 nm due to the anodic oxidation of 0-Tolidine in an acidic solution caused by the double potential step method the potential between the allows 1 and 2; 0.85 volt *vs.* SCE, the potential in the other region; 0.00 volt *vs.* SCE.

mental facts deviate from this theoretical expectation. This deviation can be attributed to the uniformity of the potential on the OTE surface, because OTE used in the experimental work has the large surface ($2 \times 7$ cm$^2$). The discrepancy of curves 1, 2, and 3 is attributed to the corrosion of the gold phase due to the electrolytic oxidation and OTE used in this experiment must be improved further.

## ACKNOWLEDGMENT

The authors are indebted to Mr. Horii of this Institute for preparing the OTE prism.

## REFERENCES

(1) N. J. Harrick, *J.P.C.*, **64**, 1110 (1960).
(2) J. Fahrenfort, *Spectrochim. Acta*, **17**, 698 (1961).
(3) N. J. Harrick, "Internal Reflection Spectroscopy," Interscience, New York (1967).
(4) W. N. Hansen in "Advances in Electrochemistry and Electrochemical Engineering," Vol. 9, P. Delahay, C. W. Tobias (eds), chap. 2, 3, John Wiley & Sons, New York (1973).
(5) N. J. Harrick and N. H. Riederman, *Spectrochim. Acta*, **21**, 2135 (1967).
(6) D. R. Tallant and D. H. Evans, *Anal. Chem.*, **41**, 835 (1969).
(7) T. Higashiyama and T. Takenaka, *J.R.C.*, **78**, 941 (1974).
(8) W. N. Hansen and J. A. Horton, *Anal. Chem.*, **36**, 783 (1964).
(9) A. Prostak, H. B. Mark, Jr., and W. N. Hansen, *J.P.C.*, **72**, 2576 (1968).
(10) T. Kuwana, in "Electroanalytical Chemistry," Vol. 7, A. J. Bard (ed.) Marcel Dekker Inc. New Nork. (1974).